



Published in final edited form as:

Free Radic Biol Med. 2022 August 01; 188: 92–102. doi:10.1016/j.freeradbiomed.2022.06.225.

Effects of sugars, fatty acids and amino acids on cytosolic and mitochondrial hydrogen peroxide release from liver cells

Jingqi Fang,

Yini Zhang,

Akos A. Gerencser,

Martin D. Brand*

Buck Institute for Research on Aging, 8001 Redwood Blvd., Novato, CA, 94945, USA

Abstract

The rates of formation of superoxide and hydrogen peroxide at different electron-donating sites in isolated mitochondria are critically dependent on the substrates that are added, through their effects on the reduction level of each site and the components of the protonmotive force. However, in intact cells the acute effects of added substrates on different sites of cytosolic and mitochondrial hydrogen peroxide production are unclear. Here we tested the effects of substrate addition on cytosolic and mitochondrial hydrogen peroxide release from intact AML12 liver cells. In 30-min starved cells replete with endogenous substrates, addition of glucose, fructose, palmitate, alanine, leucine or glutamine had no effect on the rate or origin of cellular hydrogen peroxide release. However, following 150-min starvation of the cells to deplete endogenous glycogen (and other substrates), cellular hydrogen peroxide production, particularly from NADPH oxidases (NOXs), was decreased, GSH/GSSH ratio increased, and antioxidant gene expression was unchanged. Addition of glucose or glutamine (but not the other substrates) increased hydrogen peroxide release. There were similar relative increases from each of the three major sites of production: mitochondrial sites I_Q and III_{Q_o}, and cytosolic NOXs. Glucose supplementation also restored ATP production and mitochondrial NAD reduction level, suggesting that the increased rates of hydrogen peroxide release from the mitochondrial sites were driven by increases in the protonmotive force and the degree of reduction of the electron transport chain. Long-term (24 h) glucose or glutamine deprivation also diminished hydrogen peroxide release rate, ATP production rate and (for glucose deprivation) NAD reduction level. We conclude that the rates of superoxide and hydrogen peroxide production from mitochondrial sites in liver cells are insensitive to extra added substrates when endogenous substrates are not depleted, but these rates are decreased when endogenous substrates are lowered by 150 min of starvation, and can be enhanced by restoring glucose or glutamine supply through improvements in mitochondrial energetic state.

This is an open access article under the CC BY-NC-ND license (<http://creativecommons.org/licenses/by-nc-nd/4.0/>).

*Corresponding author. mbrand@buckinstitute.org (M.D. Brand).

Appendix A. Supplementary data

Supplementary data to this article can be found online at <https://doi.org/10.1016/j.freeradbiomed.2022.06.225>.

Declaration of competing interest

Jingqi Fang, Akos Gerencser and Martin Brand were fully or partially supported by Calico LLC, South San Francisco, CA, U.S.A.

Keywords

Liver; Mitochondria; NOX; ROS; Site I_Q; Site III_{Q_o}

1. Introduction

It is half a century since mitochondria were first reported to generate superoxide and hydrogen peroxide [1–3], and there is now overwhelming evidence that mitochondria-derived superoxide and hydrogen peroxide play decisive roles in both physiological signaling and acute and chronic pathologies [4–6]. These reactive oxygen species are generated when electrons from reduced substrates, such as sugars, fatty acids and amino acids, react prematurely with molecular oxygen instead of passing down the mitochondrial electron transport chain to pump protons across the mitochondrial inner membrane and set up the protonmotive force that drives oxidative phosphorylation of ADP to ATP. Within the electron transport chain and the associated substrate dehydrogenases of mammalian mitochondria, at least 11 different sites that can generate superoxide and/or hydrogen peroxide under contrived conditions have been characterized [7].

Which of these sites run in isolated mitochondria is completely dependent on the experimental conditions, in particular which substrates are presented to the mitochondria [7–15]. The nature of the substrate determines not only which mitochondrial redox centers become reduced and hence able to pass their electrons directly to oxygen, but also the magnitude of the protonmotive force [16], which can modulate the reactivity of these reduced centers. In particular, the rate of superoxide and/or hydrogen peroxide formation at the flavin site of complex I of the electron transport chain, site I_F, is determined by the matrix NAD pool size and reduction state [17,18]. The rate at the site in complex I associated with binding of ubiquinone, site I_Q, is determined mostly by the ubiquinone (Q-pool) reduction state, and partly by the matrix NAD reduction state, and requires high protonmotive force [19,20], particularly the pH component [21]. The rate at the flavin site of complex II, site II_F, is determined by succinate concentration and Q-pool reduction [22], and the rate from the outer ubiquinone-binding site of complex III, site III_{Q_o}, is determined by Q-pool reduction and is depressed by the membrane potential component of the protonmotive force [18,23,24].

Which mitochondrial sites generate superoxide and hydrogen peroxide in cells and *in vivo*? When isolated rat skeletal muscle mitochondria were incubated in a complex medium containing the respiratory substrates found in the cytosol of resting rat skeletal muscle, at appropriate concentrations, the main sites were I_F, I_Q, II_F, and III_{Q_o} [25,26], suggesting that these sites may run in muscle cells and in skeletal muscle *in vivo*. The sites running in cultured cells can be quantified directly from the effects of specific suppressors of superoxide/hydrogen peroxide production by mitochondrial sites I_Q (S1QELs) [27,28] and III_{Q_o} (S3QELs) [29] and the effects of inhibitors of cytosolic NADPH oxidases (NOXs) (GKT136901 and ML171) [30]. This approach showed that in C2C12 cells (mouse myoblasts and myocytes) NOXs were the main hydrogen peroxide generators; the main mitochondrial generators were sites I_Q and III_{Q_o}, with site I_Q dominant in the mitochondrial

matrix [26,31]. The same was true in a range of cell lines from disparate species and tissues [32]. The protective effects of S1QELs against pathologies driven by a lack of superoxide dismutase show that site I_Q can be a significant source of superoxide *in vivo* [33]; the protective effects of S3QELs against pathological effects of a high-fat diet in the gut show the same for site III_{Q_o} [34].

It is clear from these results that mitochondrial sites I_Q and III_{Q_o} can be significant sources of superoxide and hydrogen peroxide in cells and *in vivo*, but also that the nature of the substrate can be a decisive determinant of the contributions of these sites in isolated mitochondria. What remains unclear is the extent to which acute changes in substrate supply are important determinants of the engagement of these mitochondrial sites in cells or *in vivo*. Increases in the supply of substrates such as glucose or fatty acids *in vivo* have been proposed to cause increases in the mitochondrial production of superoxide and hydrogen peroxide, as an integral step in the development of pathologies such as type II diabetes and diabetic nephropathy [35–40]. Here we investigate the dependence of mitochondrial superoxide and hydrogen peroxide production in a mouse liver cell line (AML12) on the acute and chronic manipulation of different metabolic substrates.

2. Materials and methods

2.1. Reagents

Amplex UltraRed was from ThermoFisher (Cat No. A36006); horseradish peroxidase (HRP) was from Sigma (Cat No. P8125); superoxide dismutase 1 (SOD1) was from Sigma (Cat No. S7571); NOX1/4 inhibitor ML171 was from Sigma (Cat No. 492002); S1QEL2.1 and S3QEL1.2 were provided by Calico Life Sciences LLC (South San Francisco, CA) and AbbVie Inc. (Chicago, IL). Palmitic acid (PA) was from Sigma (Cat No. P5585); fatty acid-free bovine serum albumin (BSA) was from Sigma (Cat No. A7030).

2.2. Cells

AML12 (alpha mouse liver 12) cells from ATCC were cultured under 5% (v/v) CO₂ in air at 37 °C in DMEM/F12 culture medium (Gibco, Cat No. 11320082), containing 10% (v/v) fetal bovine serum (FBS) (GeminiBio, Cat No. 100-106), 50 U/mL Penicillin-Streptomycin (Thermo Fisher, Cat No. 15070063), 1X Insulin-Transferrin-Selenium (Thermo Fisher, Cat No. 41400045), and 40 ng/ml dexamethasone (Sigma, Cat No. D4902). DMEM/F12 (Control non-deprived) culture medium was made of a non-fluorescent powder formulation of DMEM/F12 (potentiometric medium powder; a gift from Image Analyst Software (Novato, CA)) adjusted to contain 1.8 mM CaCl₂, 100 mM NaCl, 20 mM HEPES, 44 mM NaHCO₃, 1 mM pyruvate, 25 mM glucose and 10 mM glutamine; pH 7.4 at 37 °C. “Gluc-deprived” and “Gln-deprived” had glucose or glutamine omitted respectively.

2.3. Experimental design

7500 - 12,000 cells/well were seeded into 100 µL/well of DMEM/F12 culture medium in 96-well black microtiter plates (Corning, Cat No. 3340) and grown for 48 h until just confluent. They were then subjected to one of two different incubation conditions before assay of extracellular H₂O₂ release (in the presence or absence of NOX inhibitor, S1QEL or S3QEL),

oxygen consumption rate (OCR), extracellular acidification rate (ECAR), mitochondrial NAD reduction level and glycogen content.

For 30-min starvation, culture medium was replaced by KRB-BSA minimal medium (Krebs Ringer Modified Buffer (KRB): 135 mM NaCl, 5 mM KCl, 1 mM MgSO₄, 0.4 mM K₂HPO₄, 2 mM CaCl₂, 20 mM HEPES, pH 7.4 at 37 °C) with 0.1% w/v (15 μM) bovine serum albumin (BSA) for 30 min under air, then by KRB-BSA containing appropriate assay ingredients plus no substrate (control) or 25 mM glucose, 25 mM fructose, 200 μM palmitate in 33 μM BSA prepared as described [41], 10 mM alanine, 5 mM leucine or 10 mM glutamine, and assayed immediately under air. Because palmitate was added in 33 μM BSA, it was always run in parallel with a separate no-substrate control containing an additional 33 μM BSA.

For 150-min starvation, culture medium was replaced by KRB with no added substrates. Cells were incubated under air for 150 min, then the medium was replaced by KRB containing appropriate assay ingredients and substrates as for '30-min starvation' and assayed immediately.

For chronic 24-h substrate deprivation, cells were cultured for 24 h, switched to a non-fluorescent formulation of DMEM/F12 containing both 25 mM glucose and 10 mM glutamine (non-deprived), 10 mM glutamine without glucose (Gluc-deprived) or 25 mM glucose without glutamine (Gln-deprived) for 24 h, then switched into KRB and assayed immediately.

2.4. Hydrogen peroxide production rate

The rate of appearance of hydrogen peroxide in the medium and the contributions of different cytosolic and mitochondrial sites were measured as described [31,32] with slight modifications. Cells were assayed in KRB-BSA (non-starved cells) or KRB (acutely-starved cells) containing the additional assay ingredients 25 μM Amplex UltraRed, 5 U/mL horseradish peroxidase and 25 U/mL superoxide dismutase-1. Fluorescence (Ex 540 nm/Em 590 nm) was monitored using a PHERAStar FS(X) platereader. The rate was calculated as the slope of a plot of signal against time for 15–25 cycles (70 s/cycle) after subtraction of the small rate in the absence of cells in parallel wells for each experiment. The contributions of NOXs, site I_Q, and site III_{Q₀} to hydrogen peroxide release were assessed by supplementing the medium with 1 μL/mL DMSO (control), 2 μM NOX1/4 inhibitor (ML171), 1 μM S1QEL2.1 or 1 μM S3QEL1.2 in the same volume of DMSO, and calculating the difference between inhibited and control rates. The following text uses "NOXs" to indicate NOX1 and/or NOX4. Undefined sources were calculated as the difference between total and assigned sources. Hydrogen peroxide release was calibrated by addition of known amounts of hydrogen peroxide. ML171 decreased assay sensitivity, so calibrations included inhibitor as appropriate.

2.5. Glycogen content

Glycogen content was measured using a glycogen assay kit (Sigma, Cat No. MAK016). Fluorescence (Ex 540 nm/Em 590 nm) was monitored using a PHERAStar FS(X) platereader.

2.6. GSH/GSSH ratio

GSH/GSSH ratio was measured using a GSH/GSSG ratio detection assay Kit (Abcam, Cat No. ab138881). Fluorescence (Ex 490 nm/Em 520 nm) was monitored using a CLARIOstar^{plus} platereader.

2.7. RT-qPCR

Total cellular RNA was isolated using a Quick-RNA Mini-Prep (ZYMO research, Cat No. R1055). RNA samples (2 µg each) were then reverse-transcribed into cDNA using iScriptTM Reverse Transcription Supermix (BioRad, Cat No. 1708841). Quantitative real-time PCR was carried out using a Maxima SYBR Green/ROX (Thermo Fisher, Cat No. K0223) and BioRad CFX384 qPCR machine, following the manufacturer's instructions. The primers used are listed in Supplementary Table 1, and the relative levels of expression of each gene were normalized to β-actin and calculated as 2^{-CT} .

2.8. Oxygen consumption rate (OCR), extracellular acidification rate (ECAR), and ATP production rate

As described [32], 10,000 AML12 hepatocytes/well were seeded into XFe24 microplates (Agilent) and grown for 24 h or until confluent. The medium over 30-min-starved and 24-h substrate-deprived cells was replaced by KRB-BSA then the cells were incubated for 30 min (Seahorse calibration time) under air at 37 °C before assay with substrates added as indicated. The medium over 150-min-starved cells was replaced by KRB then the cells were incubated for 2 h (including Seahorse calibration time) under air at 37 °C before assay with substrates added as indicated. Rates of oxygen consumption and extracellular acidification were assessed using a Seahorse XFe24 extracellular flux analyzer (Agilent). They were normalized to cell protein in each well, then scaled to the mean control values in the first three timepoints before substrates were added. Mitochondrial respiration was assessed after subtracting rates with 1 µM rotenone plus 1 µM myxothiazol in each well. Basal rates were calculated from the last point before addition of 2 µM oligomycin. Maximal oxygen consumption rate was induced by 2 µM carbonylcyanide p-trifluoromethoxyphenylhydrazone (FCCP) and calculated as the mean of three time points. In prior experiments FCCP was added at 0.5, 1, 2, 5, and 10 µM; 2 µM was found to be optimal. Cells were lysed using 0.1% (v/v) triton X-100 and protein content was assessed using a BCA kit (Thermo Fisher, Cat No. 23235). The rate of ATP production before addition of oligomycin was calculated as described [42], using a buffering power of 0.047 for this medium [43]. Glutamine was assumed to be converted completely to lactate⁻, CO₂ and NH₄⁺ (via glutamate, succinate, oxaloacetate and pyruvate) as described by the equation $C_5H_{10}N_2O_3 + 3[O] + 3H_2O \rightarrow C_3H_5O_3^- + H^+ + 2HCO_3^- + 2NH_4^+$, which gives net H⁺/O₂ = 0.667 after accounting for ammonium and bicarbonate production and overall net P/O = 2.606 (2.364 from oxidative phosphorylation and 0.242 from substrate-linked phosphorylation in the citric acid cycle).

2.9. Mitochondrial NADH₂/NAD reduction state

The extent of mitochondrial NAD reduction was monitored as NAD(P)H₂ autofluorescence (Ex 340 nm/Em 460 nm) as described by Ref. [18] but using a PHERAStar FS(X)

platereader. Most of the signal comes from NADH₂ in the mitochondrial matrix, and NADPH₂ and cytosolic NADH₂ are assumed not to change acutely on addition of FCCP or electron transport chain inhibitors. The minimum reduction of NAD (0%) in the mitochondria was calibrated with 2 μM FCCP, and the maximum (100%) was calibrated with 1 μM rotenone plus 1 μM myxothiazol.

2.10. Statistics

Data are mean ± SEM unless SD is specified, and were analyzed by one-way ANOVA, with inter-group differences detected by Dunnett's test. ns, not significant; *p < 0.05; **p < 0.01; ***p < 0.001; ****p < 0.0001.

3. Results and discussion

3.1. Absence or presence of different added substrates does not alter hydrogen peroxide release from AML12 liver cells starved for 30 min

We examined whether acute addition of different sugars, fatty acids and amino acids affected the rate of hydrogen peroxide release from AML12 liver cells incubated for 30 min in a minimal salts medium, in the experimental design shown in Fig. 1A. The absolute rate of hydrogen peroxide appearance in the medium of cells grown in DMEM/F12 and assayed in substrate-free KRB-BSA was 89 ± 7 (SD) pmol/min/mg cell protein, similar to the value of 84 ± 5 (SD) pmol/min/mg protein produced by this cell line in the same medium in the presence of 17.5 mM glucose [32]. Fig. 1B–D shows that this rate was not significantly affected by acute addition of 25 mM glucose, 25 mM fructose, 200 μM palmitate in BSA, 10 mM alanine, 5 mM leucine or 10 mM glutamine, suggesting that the presence of endogenous substrates was sufficient to support normal production of hydrogen peroxide in these cells even in the short-term absence of added substrates. The contributions of mitochondrial sites I_Q and III_{Q_o} and cytosolic NOXs to overall hydrogen peroxide release were determined by assaying its sensitivity to acute additions of specific inhibitors of each site as described in Refs. [31,32]. Fig. 1B shows that the absolute contributions were $45.0 \pm 1.1\%$ from NOXs, $17.4 \pm 1.4\%$ from site I_Q and $20.0 \pm 1.9\%$ from site III_{Q_o}, similar to the proportions we reported previously for AML12 cells [32]. The absolute rates of these sites were not changed significantly by the addition of any of the substrates (Fig. 1B–D), and neither were their relative contributions scaled to the corresponding total rates for each substrate (Fig. 1E–G), suggesting that acute addition of substrates to these 30-min-starved cells did not affect the absolute or relative importance of any of the sites of cellular hydrogen peroxide production.

3.2. Acute addition of particular substrates to AML12 liver cells starved for 150 min partially restores hydrogen peroxide release without altering the relative contributions of individual sites

To test whether depletion of endogenous substrates could lower overall hydrogen peroxide production rates and reveal effects of subsequent acute addition of different sugars, fatty acids and amino acids, we measured the rate of hydrogen peroxide release from AML12 liver cells after acute 150-min starvation, in the experimental design shown in Fig. 2A. This short-term treatment did not alter live cell number (trypan blue assay) or the protein

content of the wells. Fig. 2B shows that cellular glycogen levels were severely depleted by 150-min-starvation, confirming that endogenous substrate reserves were indeed affected by this starvation regime. The ratio of GSH to GSSG (GSH/GSSG) is commonly used as an indicator of cellular redox status, and we measured GSH and GSSG levels (Supplementary Fig. 1) and calculated the GSH/GSSG ratio after 30-min-starvation and 150-min-starvation (Fig. 2C). As Fig. 2C shows, the GSH/GSSG ratio after 150-min-starvation was significantly higher than after 30-min-starvation. As cellular redox status is affected by oxidoreductases and enzymes involved in signaling pathways, we measured an expression panel of genes related to redox status. As shown in Supplementary Fig. 2, most of the genes were not significantly changed after 150-min-starvation compared to 30-min-starvation except *Sirtuin 1*. This may be because it will take relatively longer for the transcriptional activation of other genes in response to the redox status changes. Next, we measured the H₂O₂ production rate after 150-min fasting. Fig. 2D shows that 150-min starvation decreased the total rate of hydrogen peroxide appearance in the medium by about 40% compared to 30-min-starved cells. This decrease was not caused by increased cellular peroxidase activity, as controls showed no increase, but instead a small decrease, in the rate of clearance of an exogenous hydrogen peroxide challenge after 150-min starvation (data not shown). The only significant contributors to the decrease of the absolute rate were the NOXs (Fig. 2D). Fig. 2E shows that, when rescaled as % of total rate in each condition, the relative contribution of NOXs was significantly decreased by acute starvation, and the relative contributions of sites I_Q and III_{Q_o} were correspondingly increased. Thus acute 150-min-starvation depletes the glycogen stores in these liver cells, and (perhaps because the pentose phosphate pathway is provided with less glucose 6-phosphate to generate NADPH) NADPH oxidases run more slowly but the two mitochondrial sites are not greatly affected. Therefore, and consistently with the observed decreased peroxidase activity, the observed increased GSH/GSSH ratio is expected to be a result of decreased H₂O₂ production. Furthermore, the decreased total cellular H₂O₂ production cannot be due to increased scavenging by a panel of antioxidant pathways.

We then tested whether acute addition of different substrates could restore hydrogen peroxide release from these 150-min-starved cells, and if so, which sites were increased. Fig. 2F–H shows that the overall rate of hydrogen peroxide release was significantly increased by acute addition of glucose (Fig. 2F) or glutamine (Fig. 2H), although not completely restored to the rates exhibited by non-starved cells (compare Fig. 2D). The overall rates from 150-min-starved cells were not significantly increased by fructose, palmitate, alanine, or leucine. The contributions of mitochondrial sites I_Q and III_{Q_o} and cytosolic NOXs to overall hydrogen peroxide release were determined as above. Fig. 2F–H shows that the absolute contributions from all sites were increased significantly by addition of glucose (Fig. 2F) or (for site I_Q) glutamine (Fig. 2H) but not by the other substrates. Fig. 2I–K shows the relative contributions scaled to the corresponding total rates for each substrate (Fig. 2F–H); despite partial restoration of the total rates of hydrogen peroxide release by 150-min-starved cells following acute addition of glucose or glutamine, none of the sites altered its relative contribution. Thus, acute addition of glucose or glutamine to these 150-min-starved cells partially restored the absolute rates of hydrogen peroxide release, but did so by stimulating all sites to about the same extent. The other substrates tested did not restore hydrogen peroxide release, perhaps because they were less readily metabolized.

3.3. 24-h deprivation of glucose or glutamine diminishes hydrogen peroxide release and alters the contributions of individual sites

To test the longer-term effects of specific substrates on hydrogen peroxide release, we omitted individual substrates from the culture medium for 24 h. Fig. 2 shows that after 150-min starvation only addition of glucose or glutamine significantly increased hydrogen peroxide release, so we tested the effects of 24-h glucose or glutamine deprivation (Fig. 3). We cultured cells for 24 h, then switched them to DMEM/F12 containing both 25 mM glucose and 10 mM glutamine (non-deprived) or 10 mM glutamine without glucose (gluc-deprived) or 25 mM glucose without glutamine (gln-deprived) for 24 h, then switched them into KRB and assayed immediately (Fig. 3A). Overall hydrogen peroxide release dropped significantly after 24-h deprivation of glucose or glutamine (Fig. 3B). Under glucose deprivation, all of the sites (I_Q , III_{Q_0} and NOXs) slowed significantly whereas under glutamine deprivation, only the NOXs slowed significantly (Fig. 3C), suggesting that glutamine may be the main substrate driving hydrogen peroxide generation in the cytosol. Fig. 3D and E shows the effects on the relative contributions of the different sites. Since the cells were deprived of glucose or glutamine for 24 h, the expression of many genes may have changed adaptively, potentially altering the bioenergetic and redox networks and making it hard to separate out the underlying mechanisms.

3.4. The rate of ATP production as a proxy for the bioenergetic state of AML12 cells during substrate manipulation

To probe the extent of metabolic disturbance caused by substrate manipulation, we determined the rate of cellular ATP production as a proxy for the energetic state of the mitochondria. 30-min-starved, 150-min-starved, and 24-h-deprived AML12 cells were subjected to a standard cell respiratory control experiment [44] in minimal medium in a Seahorse extracellular flux analyzer, and the rates of ATP production by oxidative phosphorylation and glycolysis after addition of vehicle, glucose or glutamine were calculated from the observed rates of oxygen consumption and extracellular acidification [42,45] (Fig. 4).

Addition of glutamine to 30-min-starved AML12 cells had little effect or moderately increased oxygen consumption rate (Fig. 4A) and lowered extracellular acidification rate (Fig. 4B), and made no significant change to the rate of, or the contributors to, ATP production (Fig. 4C).

Addition of glucose to 30-min-starved AML12 cells depressed oxygen consumption rate (Fig. 4A) and oxidative ATP production rate (Fig. 4C) and stimulated extracellular acidification rate (Fig. 4B), and glycolytic ATP production rate (Fig. 4C). There was no change in the total ATP production rate. This is the Crabtree effect; the suppression of oxidative phosphorylation by ATP supplied by glycolysis [42,46]. These results reinforce the conclusion reached in section 3.1 that 30-min-starved AML12 cells retain sufficient endogenous substrates to satisfy their energetic requirements, and show little response to added substrates other than increasing glycolytic ATP production rate and correspondingly slowing oxidative ATP production rate when glucose is present.

Compared to 30-min-starved cells, 150-min-starved cells without added substrates had depressed basal rates of oxygen consumption (Fig. 4D), extracellular acidification (Fig. 4E) and ATP production (Fig. 4F), consistent with the depletion of endogenous glycogen (Fig. 2B) and presumably other endogenous substrates. Their energetics were strongly responsive to the addition of glucose or glutamine. Acute addition of glucose after 150-min-starvation triggered a very strong Crabtree effect, with depressed oxygen consumption rate (Fig. 4D) and oxidative ATP production rate (Fig. 4F) and stimulated extracellular acidification rate (Fig. 4E), and glycolytic and total ATP production rate (Fig. 4F). Acute addition of glutamine stimulated basal (and maximal) oxygen consumption rate (Fig. 4D) and oxidative and total ATP production rate (Fig. 4F). These effects indicate that the addition of glucose or glutamine improved the mitochondrial energetic state of 150-min-starved cells by providing mitochondrial substrates (pyruvate and glutamine respectively), which is expected to lead directly to a greater reduction of the electron transport chain, greater protonmotive force, and hence greater hydrogen peroxide production. In addition, glucose also drove glycolytic ATP production, which spared oxidative phosphorylation, and again, this is expected to lead to greater protonmotive force, greater reduction of the electron transport chain and greater hydrogen peroxide production. These improvements in energetic state are plausible candidates for the restored hydrogen peroxide production seen in Fig. 2E,G.

Compared to 'non-deprived', 24-h glucose or glutamine deprivation caused depressed basal rates of oxygen consumption (Fig. 4G), extracellular acidification (Fig. 4H) and ATP production (Fig. 4I), which suggests that at least some of the effects of 24-h substrate deprivation on hydrogen peroxide release rates (Fig. 3) may be caused by energetic effects (lower protonmotive force and lower reduction of respiratory chain components). However, putative changes in gene expression make this suggestion tentative at best.

3.5. Glucose or glutamine effects on the reduction level of mitochondrial NAD

In section 3.4 we interpreted the changes in the rate of ATP turnover in Fig. 4F as driven by changes in ATP supply dependent on substrate availability. However, in principle ATP production might instead have been stimulated by the demand for ATP to process the added substrates, for example, for repletion of cellular glycogen. This would be accompanied by a lower protonmotive force and decreased reduction of the electron transport chain. To distinguish between these possibilities and to explore energetics further, we measured the reduction level of the mitochondrial NAD pool using autofluorescence. Fig. 5A and B shows that in 30-min-starved cells, the mitochondrial NAD signal was about 50% reduced, and addition of glucose or glutamine had no effect. However, in 150-min-starved cells (Fig. 5C and D), the mitochondrial NAD signal was only about 15% reduced, consistent with the depletion of endogenous glycogen (Fig. 2B) and other endogenous substrates. Acute addition of glucose or glutamine significantly restored the reduction level of the mitochondrial NAD (Fig. 5C and D). 24-h glucose-deprivation caused a depressed reduction level of mitochondrial NAD (Fig. 5E and F), but glutamine-deprivation did not (Fig. 5E and F), which is consistent with long-term glutamine deprivation lowering only hydrogen peroxide from the cytosolic NOXs (Fig. 3C). These effects are those predicted for a limitation of electron supply rather than a limitation of ATP demand during acute starvation.

Conversely, after acute addition of substrates, restoration of electron supply rather than increased ATP demand is consistent with the conclusions drawn in section 3.4.

6. Conclusions

We conclude that the rates of superoxide and hydrogen peroxide production from cytosolic and mitochondrial sites in 30-min-starved AML12 liver cells switched into a minimal medium are insensitive to the presence or absence of common substrates in the assay medium. As summarized by Fig. 6, we infer that endogenous substrates are adequate to keep cytosolic NADP sufficiently reduced to maintain hydrogen peroxide production from NOXs, and to keep the mitochondrial electron transport chain sufficiently reduced and the proton motive force sufficiently high to maintain a high rate of oxidative ATP production and high rates of superoxide/hydrogen peroxide production from mitochondrial sites I_Q and III_{Q_o}.

However, in 150-min-starved AML12 liver cells the rates of superoxide and hydrogen peroxide production from mitochondrial sites are decreased because of inadequate substrate availability, as evidenced by slowed rates of ATP production and a lowered reduction level of mitochondrial NAD. Furthermore, this decrease was not due to increased peroxidase activity or to changes to other scavenging pathways, and GSH/GSSG was likely increased as a result of lowered oxidation. Addition of glucose (or to some extent glutamine), but not the other substrates tested, raises cytosolic NADP reduction and mitochondrial NAD and Q reduction, leading to increased protonmotive force. The increased cytosolic NADP reduction state partially restores hydrogen peroxide production from NOXs, and the improvements in mitochondrial energetic state restore rates of ATP production, and increase the rates of superoxide and hydrogen peroxide production from sites I_Q and III_{Q_o} of the mitochondrial electron transport chain.

Similar effects occurred in cells depleted of glucose or glutamine for 24 h. Deprivation of glucose decreased hydrogen peroxide release from all three sites, whereas deprivation of glutamine decreased only the contribution of NOXs. The effects on mitochondrial sites may be partially caused by changes in energetics, but gene expression changes cloud the interpretation in the 24-h deprivation model.

30-min-starved liver cells in minimal medium have sufficient endogenous substrates to drive hydrogen peroxide release, and, unlike isolated mitochondria [11], this release is insensitive to the presence or absence of external sugars, fatty acids or amino acids. Only when endogenous substrates are depleted by deprivation of extracellular substrates for 150 min do the cells respond to acute additions of glucose or glutamine. Liver cells are specialized by having the metabolic flexibility to maintain circulating substrates for other tissues [47], so 30-min-starved liver cells may be exceptional in not altering their hydrogen peroxide release when presented with additional exogenous substrates. Whether this is the case in cells from other tissues has yet to be explored.

Supplementary Material

Refer to Web version on PubMed Central for supplementary material.

Acknowledgements

We thank Chad Lerner for technical assistance.

Funding

This work was supported by Calico Life Sciences LLC (South San Francisco, CA) and the Buck Institute for Research on Aging (Novato, CA). Some aspects were supported by the National Institutes of Health (NIH) grant 1R41DA043369 to AAG. These sponsors had no involvement in study design, the collection, analysis and interpretation of data, the writing of the report, or the decision to submit the article for publication.

Abbreviations:

NOX	NADPH oxidase
Q	ubiquinone
Site I_F	mitochondrial site of superoxide and/or hydrogen peroxide production associated with the flavin of complex I
Site I_Q	mitochondrial site of superoxide and/or hydrogen peroxide production associated with the quinone-binding site of complex I
Site II_F	mitochondrial site of superoxide and/or hydrogen peroxide production associated with the flavin of complex II
Site III_{Q_o}	mitochondrial site of superoxide production associated with the outer quinone-binding site of complex III

References

- [1]. Jensen PK, Antimycin-insensitive oxidation of succinate and reduced nicotinamide-adenine dinucleotide in electron-transport particles. I. pH dependency and hydrogen peroxide formation, *Biochim. Biophys. Acta* 122 (1966) 157–166. <https://www.ncbi.nlm.nih.gov/pubmed/4291041>. [PubMed: 4291041]
- [2]. Boveris A, Chance B, The mitochondrial generation of hydrogen peroxide. General properties and effect of hyperbaric oxygen, *Biochem. J* 134 (1973) 707–716. <http://www.ncbi.nlm.nih.gov/pubmed/4749271>. [PubMed: 4749271]
- [3]. Boveris A, Cadenas E, Mitochondrial production of superoxide anions and its relationship to the antimycin insensitive respiration, *FEBS Lett.* 54 (1975) 311–314. <http://www.ncbi.nlm.nih.gov/pubmed/236930>. [PubMed: 236930]
- [4]. Diebold L, Chandel NS, Mitochondrial ROS regulation of proliferating cells, *Free Rad. Biol. Med* 100 (2016) 86–93. <https://www.ncbi.nlm.nih.gov/pubmed/27154978>. [PubMed: 27154978]
- [5]. Brand MD, Riding the tiger - physiological and pathological effects of superoxide and hydrogen peroxide generated in the mitochondrial matrix, *Crit. Rev. Biochem. Mol. Biol* 55 (2020) 592–661. <https://www.ncbi.nlm.nih.gov/pubmed/33148057>. [PubMed: 33148057]
- [6]. Sies H, Jones DP, Reactive oxygen species (ROS) as pleiotropic physiological signalling agents, *Nat. Rev. Mol. Cell Biol* 21 (2020) 363–383. <https://www.ncbi.nlm.nih.gov/pubmed/32231263>. [PubMed: 32231263]
- [7]. Brand MD, Mitochondrial generation of superoxide and hydrogen peroxide as the source of mitochondrial redox signaling, *Free Rad. Biol. Med* 100 (2016) 14–31. <https://www.ncbi.nlm.nih.gov/pubmed/27085844>. [PubMed: 27085844]

- [8]. Hansford RG, Hogue BA, Mildaziene V, Dependence of H₂O₂ formation by rat heart mitochondria on substrate availability and donor age, *J. Bioenerg. Biomembr* 29 (1997) 89–95. <http://www.ncbi.nlm.nih.gov/pubmed/9067806>. [PubMed: 9067806]
- [9]. Orr AL, Quinlan CL, Perevoshchikova IV, Brand MD, A refined analysis of superoxide production by mitochondrial sn-glycerol 3-phosphate dehydrogenase, *J. Biol. Chem* 287 (2012) 42921–42935. <http://www.ncbi.nlm.nih.gov/pubmed/23124204>. [PubMed: 23124204]
- [10]. Perevoshchikova IV, Quinlan CL, Orr AL, Gerencser AA, Brand MD, Sites of superoxide and hydrogen peroxide production during fatty acid oxidation in rat skeletal muscle mitochondria, *Free Rad. Biol. Med* 61 (2013) 298–309. <http://www.ncbi.nlm.nih.gov/pubmed/23583329>. [PubMed: 23583329]
- [11]. Quinlan CL, Perevoshchikova IV, Hey-Mogensen M, Orr AL, Brand MD, Sites of reactive oxygen species generation by mitochondria oxidizing different substrates, *Redox Biol.* 1 (2013) 304–312. <http://www.ncbi.nlm.nih.gov/pubmed/24024165> <http://www.ncbi.nlm.nih.gov/pmc/articles/PMC3757699/pdf/main.pdf>. [PubMed: 24024165]
- [12]. Goncalves RL, Rothschild DE, Quinlan CL, Scott GK, Benz CC, Brand MD, Sources of superoxide/H₂O₂ during mitochondrial proline oxidation, *Redox Biol.* 2 (2014) 901–909. <http://www.ncbi.nlm.nih.gov/pubmed/25184115>. [PubMed: 25184115]
- [13]. Hey-Mogensen M, Goncalves RL, Orr AL, Brand MD, Production of superoxide/H₂O₂ by dihydroorotate dehydrogenase in rat skeletal muscle mitochondria, *Free Rad. Biol. Med* 72 (2014) 149–155. <http://www.ncbi.nlm.nih.gov/pubmed/24746616>. [PubMed: 24746616]
- [14]. Quinlan CL, Goncalves RL, Hey-Mogensen M, Yadava N, Bunik VI, Brand MD, The 2-oxoacid dehydrogenase complexes in mitochondria can produce superoxide/hydrogen peroxide at much higher rates than complex I, *J. Biol. Chem* 289 (2014) 8312–8325. <https://www.ncbi.nlm.nih.gov/pubmed/24515115>. [PubMed: 24515115]
- [15]. Goncalves RLS, Bunik VI, Brand MD, Production of superoxide/hydrogen peroxide by the mitochondrial 2-oxoadipate dehydrogenase complex, *Free Rad. Biol. Med* 91 (2016) 247–255, 10.1016/j.freeradbiomed.2015.12.020. [PubMed: 26708453]
- [16]. Mookerjee SA, Gerencser AA, Watson MA, Brand MD, Controlled power: how biology manages succinate-driven energy release, *Biochem Soc Trans* (2021), 10.1042/BST20211032. BST20211032.
- [17]. Kussmaul L, Hirst J, The mechanism of superoxide production by NADH: ubiquinone oxidoreductase (complex I) from bovine heart mitochondria, *Proc. Nat. Acad. Sci. U. S. A* 103 (2006) 7607–7612. <http://www.ncbi.nlm.nih.gov/pubmed/16682634>.
- [18]. Quinlan CL, Treberg JR, Perevoshchikova IV, Orr AL, Brand MD, Native rates of superoxide production from multiple sites in isolated mitochondria measured using endogenous reporters, *Free Rad. Biol. Med* 53 (2012) 1807–1817. <http://www.ncbi.nlm.nih.gov/pubmed/22940066>. [PubMed: 22940066]
- [19]. Treberg JR, Quinlan CL, Brand MD, Evidence for two sites of superoxide production by mitochondrial NADH-ubiquinone oxidoreductase (complex I), *J. Biol. Chem* 286 (2011) 27103–27110. <http://www.ncbi.nlm.nih.gov/pubmed/21659507>. [PubMed: 21659507]
- [20]. Robb EL, Hall AR, Prime TA, Eaton S, Szibor M, Viscomi C, James AM, Murphy MP, Control of mitochondrial superoxide production by reverse electron transport at complex I, *J. Biol. Chem* 293 (2018) 9869–9879. <https://www.ncbi.nlm.nih.gov/pubmed/29743240>. [PubMed: 29743240]
- [21]. Lambert AJ, Brand MD, Superoxide production by NADH:ubiquinone oxidoreductase (complex I) depends on the pH gradient across the mitochondrial inner membrane, *Biochem. J* 382 (2004) 511–517. <http://www.ncbi.nlm.nih.gov/pubmed/15175007>. [PubMed: 15175007]
- [22]. Quinlan CL, Orr AL, Perevoshchikova IV, Treberg JR, Ackrell BA, Brand MD, Mitochondrial complex II can generate reactive oxygen species at high rates in both the forward and reverse reactions, *J. Biol. Chem* 287 (2012) 27255–27264. <http://www.ncbi.nlm.nih.gov/pubmed/22689576>. [PubMed: 22689576]
- [23]. Drose S, Brandt U, The mechanism of mitochondrial superoxide production by the cytochrome *bc*₁ complex, *J. Biol. Chem* 283 (2008) 21649–21654. <http://www.ncbi.nlm.nih.gov/pubmed/18522938>. [PubMed: 18522938]

- [24]. Quinlan CL, Gerencser AA, Treberg JR, Brand MD, The mechanism of superoxide production by the antimycin-inhibited mitochondrial Q-cycle, *J. Biol. Chem* 286 (2011) 31361–31372. <https://www.ncbi.nlm.nih.gov/pubmed/21708945>. [PubMed: 21708945]
- [25]. Goncalves RL, Quinlan CL, Perevoshchikova IV, Hey-Mogensen M, Brand MD, Sites of superoxide and hydrogen peroxide production by muscle mitochondria assessed *ex vivo* under conditions mimicking rest and exercise, *J. Biol. Chem* 290 (2015) 209–227. <http://www.ncbi.nlm.nih.gov/pubmed/25389297>. [PubMed: 25389297]
- [26]. Goncalves RLS, Watson MA, Wong HS, Orr AL, Brand MD, The use of site-specific suppressors to measure the relative contributions of different mitochondrial sites to skeletal muscle superoxide and hydrogen peroxide production, *Redox Biol.* 28 (2020), 101341. <https://www.ncbi.nlm.nih.gov/pubmed/31627168>. [PubMed: 31627168]
- [27]. Orr AL, Ashok D, Sarantos MR, Shi T, Hughes RE, Brand MD, Inhibitors of ROS production by the ubiquinone-binding site of mitochondrial complex I identified by chemical screening, *Free Rad. Biol. Med* 65 (2013) 1047–1059. <http://www.ncbi.nlm.nih.gov/pubmed/23994103>. [PubMed: 23994103]
- [28]. Brand MD, Goncalves RL, Orr AL, Vargas L, Gerencser AA, Borch Jensen M, Wang YT, Melov S, Turk CN, Matzen JT, Dardov VJ, Petrassi HM, Meeusen SL, Perevoshchikova IV, Jasper H, Brookes PS, Ainscow EK, Suppressors of superoxide-H₂O₂ production at site I_Q of mitochondrial Complex I protect against stem cell hyperplasia and ischemia-reperfusion injury, *Cell Metabol.* 24 (2016) 582–592. <https://www.ncbi.nlm.nih.gov/pubmed/27667666>.
- [29]. Orr AL, Vargas L, Turk CN, Baaten JE, Matzen JT, Dardov VJ, Atde SJ, Li J, Quackenbush DC, Goncalves RLS, Perevoshchikova IV, Petrassi HM, Meeusen SL, Ainscow EK, Brand MD, Suppressors of superoxide production from mitochondrial complex III, *Nat. Chem. Biol* 11 (2015) 834–836. <http://www.ncbi.nlm.nih.gov/pubmed/26368590>. [PubMed: 26368590]
- [30]. Cifuentes-Pagano ME, Meijles DN, Pagano PJ, Nox inhibitors & therapies: rational design of peptidic and small molecule inhibitors, *Curr. Pharmaceut. Des* 21 (2015) 6023–6035. <https://www.ncbi.nlm.nih.gov/pubmed/26510437>.
- [31]. Wong HS, Benoit B, Brand MD, Mitochondrial and cytosolic sources of hydrogen peroxide in resting C2C12 myoblasts, *Free Rad. Biol. Med* 130 (2018) 140–150. <https://www.ncbi.nlm.nih.gov/pubmed/30389498>. [PubMed: 30389498]
- [32]. Fang J, Wong HS, Brand MD, Production of superoxide and hydrogen peroxide in the mitochondrial matrix is dominated by site I_Q of complex I in diverse cell lines, *Redox Biol.* 37 (2020), 101722. <https://www.ncbi.nlm.nih.gov/pubmed/32971363>. [PubMed: 32971363]
- [33]. Wong HS, Mezera V, Dighe P, Melov S, Gerencser AA, Sweis RF, Pliushchev M, Wang Z, Esbenshade T, McKibben B, Riedmaier S, Brand MD, Superoxide produced by mitochondrial site I_Q inactivates cardiac succinate dehydrogenase and induces hepatic steatosis in Sod2 knockout mice, *Free Rad. Biol. Med* 164 (2021) 223–232, 10.1016/j.freeradbiomed.2020.12.447. [PubMed: 33421588]
- [34]. Watson MA, Pattavina B, Hilsabeck TAU, Lopez-Dominguez J, Kapahi P, Brand MD, S3QELs protect against diet-induced intestinal barrier dysfunction, *Aging Cell* 20 (2021), e13476. <https://www.ncbi.nlm.nih.gov/pubmed/34521156>. [PubMed: 34521156]
- [35]. Brownlee M, The pathobiology of diabetic complications: a unifying mechanism, *Diabetes* 54 (2005) 1615–1625. <http://www.ncbi.nlm.nih.gov/pubmed/15919781>. [PubMed: 15919781]
- [36]. Quagliaro L, Piconi L, Assaloni R, Da Ros R, Szabo C, Ceriello A, Primary role of superoxide anion generation in the cascade of events leading to endothelial dysfunction and damage in high glucose treated HUVEC, *Nutr. Metabol. Cardiovasc. Dis* 17 (2007) 257–267. <https://www.ncbi.nlm.nih.gov/pubmed/16891102>.
- [37]. Liemburg-Apers DC, Willems PH, Koopman WJ, Grefte S, Interactions between mitochondrial reactive oxygen species and cellular glucose metabolism, *Arch. Toxicol* 89 (2015) 1209–1226. <https://www.ncbi.nlm.nih.gov/pubmed/26047665>. [PubMed: 26047665]
- [38]. Nishikawa T, Brownlee M, Araki E, Mitochondrial reactive oxygen species in the pathogenesis of early diabetic nephropathy, *J. Diabetes Invest* 6 (2015) 137–139. <http://www.ncbi.nlm.nih.gov/pubmed/25802720>.

- [39]. Lee E, Choi J, Lee HS, Palmitate induces mitochondrial superoxide generation and activates AMPK in podocytes, *J. Cell. Physiol* 232 (2017) 3209–3217. <https://www.ncbi.nlm.nih.gov/pubmed/28214337>. [PubMed: 28214337]
- [40]. Newsholme P, Keane KN, Carlessi R, Cruzat V, Oxidative stress pathways in pancreatic beta-cells and insulin-sensitive cells and tissues: importance to cell metabolism, function, and dysfunction, *Am. J. Physiol. Cell Physiol* 317 (2019) C420–C433. <https://www.ncbi.nlm.nih.gov/pubmed/31216193>. [PubMed: 31216193]
- [41]. Pike Winer LS, Wu M, Rapid analysis of glycolytic and oxidative substrate flux of cancer cells in a microplate, *PLoS One* 9 (2014), e109916. <https://www.ncbi.nlm.nih.gov/pubmed/25360519>. [PubMed: 25360519]
- [42]. Mookerjee SA, Gerencser AA, Nicholls DG, Brand MD, Quantifying intracellular rates of glycolytic and oxidative ATP production and consumption using extracellular flux measurements, *J. Biol. Chem* 292 (2017) 7189–7207. <https://www.ncbi.nlm.nih.gov/pubmed/28270511>, <https://doi.org/10.1074/jbc.AAC118.004855>. Errata: *J Biol Chem* 293:12649-12652; 2018. [PubMed: 28270511]
- [43]. Mookerjee SA, Brand MD, Measurement and analysis of extracellular acid production to determine glycolytic rate, *J. Vis. Exp* (2015), e53464. <https://www.ncbi.nlm.nih.gov/pubmed/26709455>. [PubMed: 26709455]
- [44]. Brand MD, Nicholls DG, Assessing mitochondrial dysfunction in cells, *Biochem. J* 435 (2011) 297–312. <http://www.ncbi.nlm.nih.gov/pubmed/21726199>. [PubMed: 21726199]
- [45]. Louie MC, Ton J, Brady ML, Le DT, Mar JN, Lerner CA, Gerencser AA, Mookerjee SA, Total cellular ATP production changes with primary substrate in MCF7 breast cancer cells, *Front. Oncol* 10 (2020) 1703. <https://www.ncbi.nlm.nih.gov/pubmed/33224868>. [PubMed: 33224868]
- [46]. Ibsen KH, The Crabtree effect: a review, *Cancer Res.* 21 (1961) 829–841. <https://www.ncbi.nlm.nih.gov/pubmed/13717358>. [PubMed: 13717358]
- [47]. Randle PJ, Metabolic fuel selection: general integration at the whole-body level, *Proc. Nutr. Soc* 54 (1995) 317–327. <https://www.ncbi.nlm.nih.gov/pubmed/7568263>. [PubMed: 7568263]

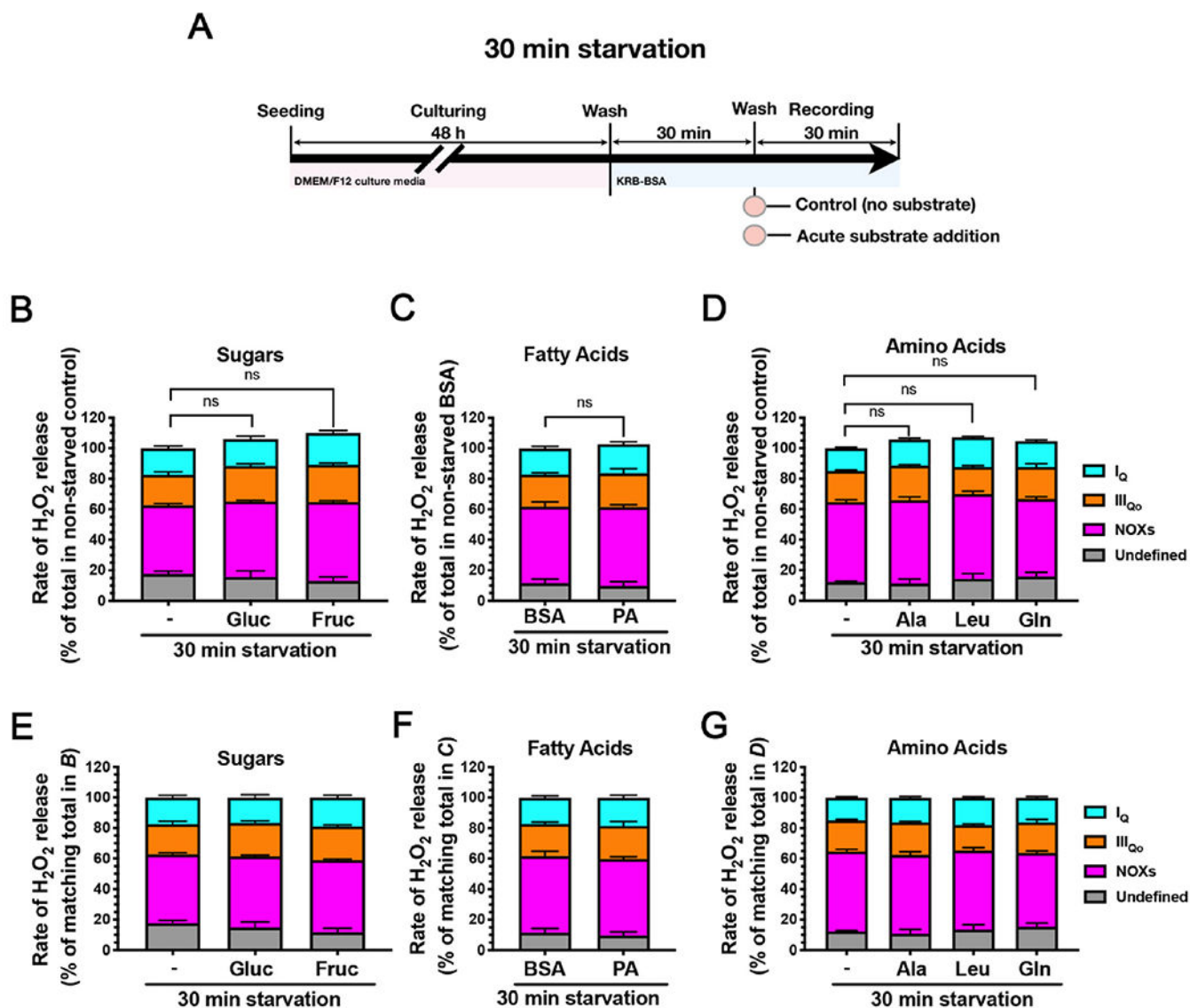


Fig. 1. Effects of acute addition of different substrates on rates of hydrogen peroxide release from 30-min-starved AML12 cells. (A) AML12 cells were grown in DMEM/F12 medium. “Wash” indicates that this medium was replaced by KRB-BSA medium for 30 min, then replaced by KRB-BSA containing no substrate (control, marked ‘-’ in *B,D,E,G*, or control containing 33 μ M BSA in *C,F*) or the substrates indicated in *B-G* (pink circles) and immediately assayed for 30 min for the rate of appearance of extracellular hydrogen peroxide in the absence (to define total rate) or presence of S1QEL, S3QEL or NOX inhibitor (to define the contributions of individual sites). (B–D) Total hydrogen peroxide release rates (heights of stacked columns) scaled to the relevant no-substrate control, and contributions of site I_Q, site III_{Q0}, NOXs, and undefined sources (colored boxes) after acute addition of (B) sugars (Gluc, 25 mM glucose, Fruc, 25 mM fructose), (C) fatty acid (33 μ M BSA with 200 μ M PA, palmitate) and (D) amino acids (10 mM alanine, 5 mM leucine, 10 mM glutamine). (E–G) Contributions of site I_Q, site III_{Q0}, NOXs and undefined sources

scaled to each corresponding total rate in *B-D*. The total hydrogen peroxide release rates in *B-D* were not significantly different between each substrate and the relevant control (ns, not significant). The contributions (*B-D*) and relative proportions (*E-G*) from each site (same color boxes) were not significantly different from their values in the relevant no-substrate control. Values are means \pm SEM (N = 3 independent experiments each the mean of three biological replicates). (For interpretation of the references to color in this figure legend, the reader is referred to the Web version of this article.)

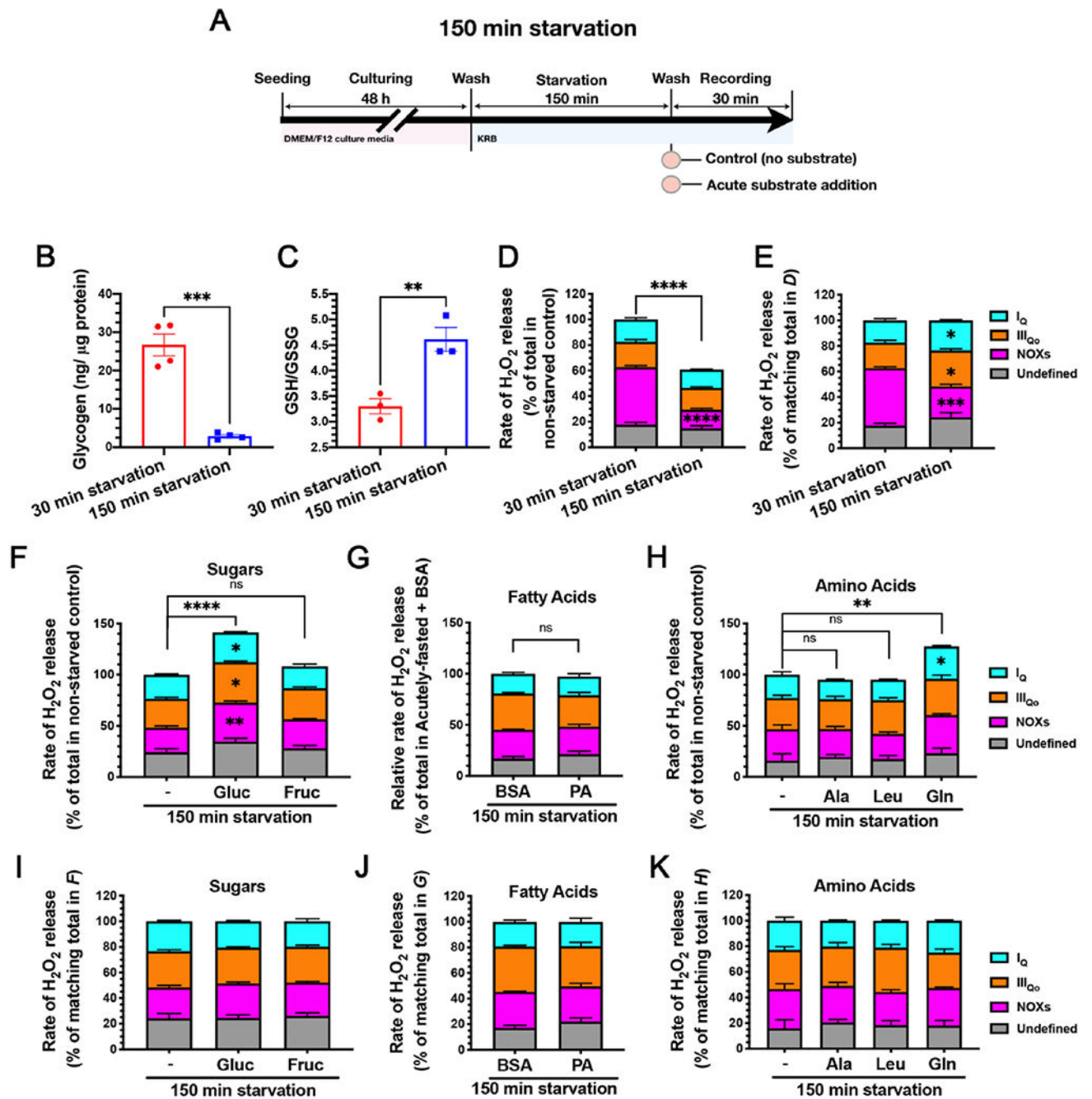


Fig. 2. Effects of acute addition of different substrates on rates of hydrogen peroxide release from 150-min-starved AML12 cells. (A) AML12 cells were grown in DMEM/F12 medium. “Wash” indicates that this medium was replaced by KRB containing no substrate for 150 min, then by KRB containing no substrate (control, marked ‘-’ in *F*, *H*, *I*, *K*, or control containing 33 μM BSA in *G*, *J*) or the substrates indicated in *F*–*K* (pink circles). The rates of appearance of extracellular hydrogen peroxide were then recorded for 30 min in the absence (to define total rate) or presence of S1QEL, S3QEL or NOX inhibitor (to

define the contributions of individual sites). (B) Glycogen levels in 30 min-starved and 150-min-starved cells. (C) GSH/GSSG ratios in 30 min-starved and 150-min-starved cells. (D) Total hydrogen peroxide release rates (heights of stacked columns) scaled to the non-starved control and contributions of site I_Q, site III_{Q_o}, NOXs, and undefined sources (colored boxes). (E) Relative contributions of site I_Q, site III_{Q_o} and NOXs scaled to the corresponding total rate in *D*. (F–H) Total hydrogen peroxide release rates (heights of stacked columns) scaled to the relevant no-substrate control and contributions of site I_Q, site III_{Q_o}, NOXs, and undefined sources (colored boxes) after acute addition of (F) sugars (Gluc, 25 mM glucose, Fruc, 25 mM fructose), (G) fatty acid (33 μM BSA with 200 μM PA, palmitate) and (H) amino acids (10 mM alanine, 5 mM leucine, 10 mM glutamine). (I–K) Contributions of site I_Q, site III_{Q_o}, NOXs and undefined sources scaled to each corresponding total rate in *F–H*. Values are means ± SEM (N = 3 independent experiments each the mean of three biological replicates). (For interpretation of the references to color in this figure legend, the reader is referred to the Web version of this article.)

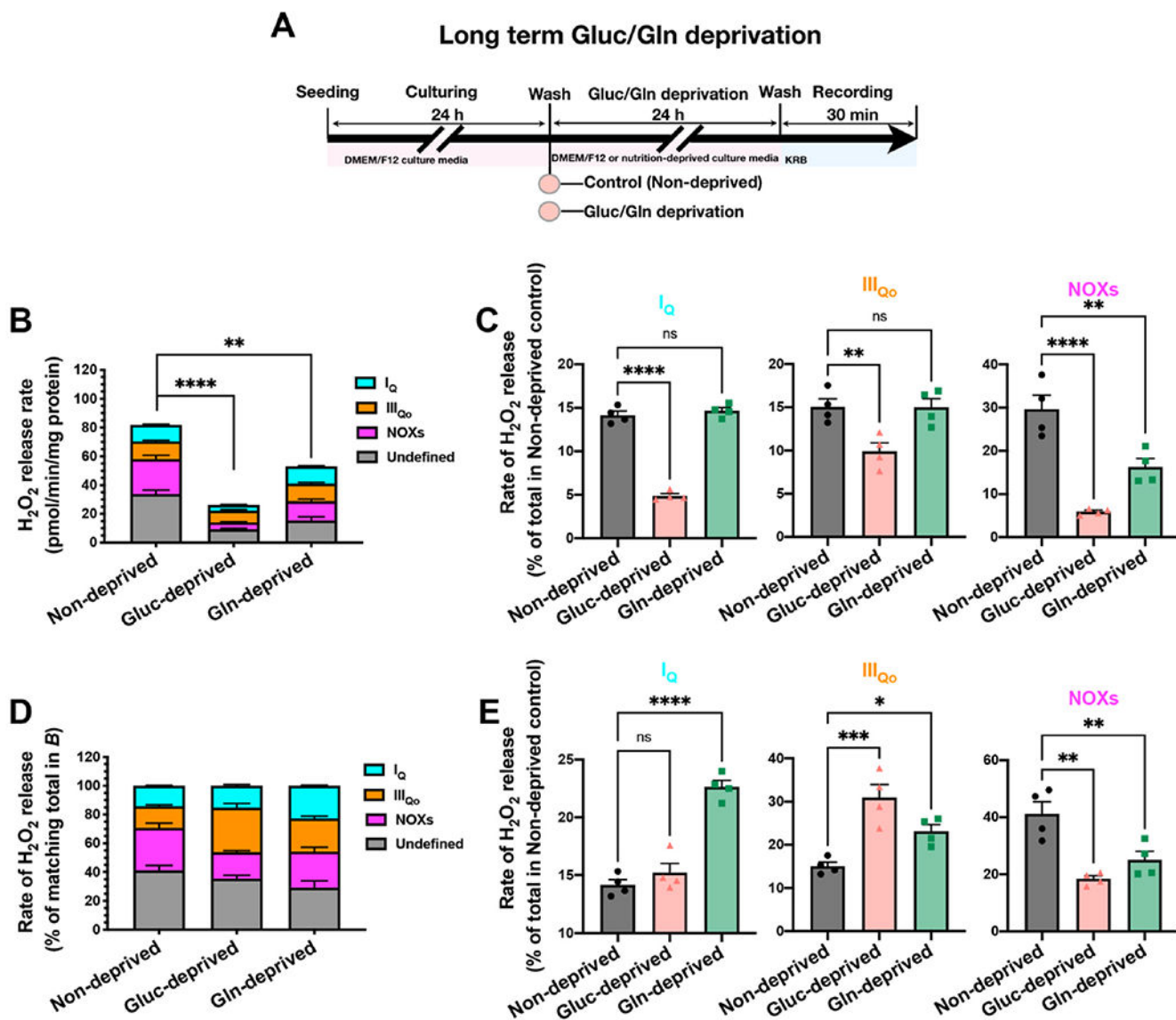


Fig. 3. Effects of 24-h glucose or glutamine deprivation on rates of hydrogen peroxide release from AML12 cells. (A) AML12 cells were grown in DMEM/F12 medium for 24 h. “Wash” indicates that this medium was replaced by a non-fluorescent formulation of DMEM/F12 containing both 25 mM glucose and 10 mM glutamine (non-deprived), 10 mM glutamine without glucose (Gluc-deprived) or 25 mM glucose without glutamine (Gln-deprived) for 24 h, then switched into KRB and assayed immediately. (B) Total hydrogen peroxide release rates (heights of stacked columns) and contributions of site I_Q, site III_{QO}, NOXs, and undefined sources (colored boxes) after 24 h culture (non-deprived), 24-h glucose deprivation (Gluc-deprived), or 24-h glutamine deprivation (Gln-deprived). (C) Statistical analysis of the absolute rates from sites I_Q, III_{QO} and NOXs shown in B. (D) Relative contributions of site I_Q, site III_{QO} and NOXs scaled to the corresponding total rate in C. (E)

Statistical analysis of the relative rates from sites I_Q, III_{Q₀} and NOXs shown in *D*. Values are means \pm SEM (N = 3 independent experiments each the mean of three biological replicates).

Author Manuscript

Author Manuscript

Author Manuscript

Author Manuscript

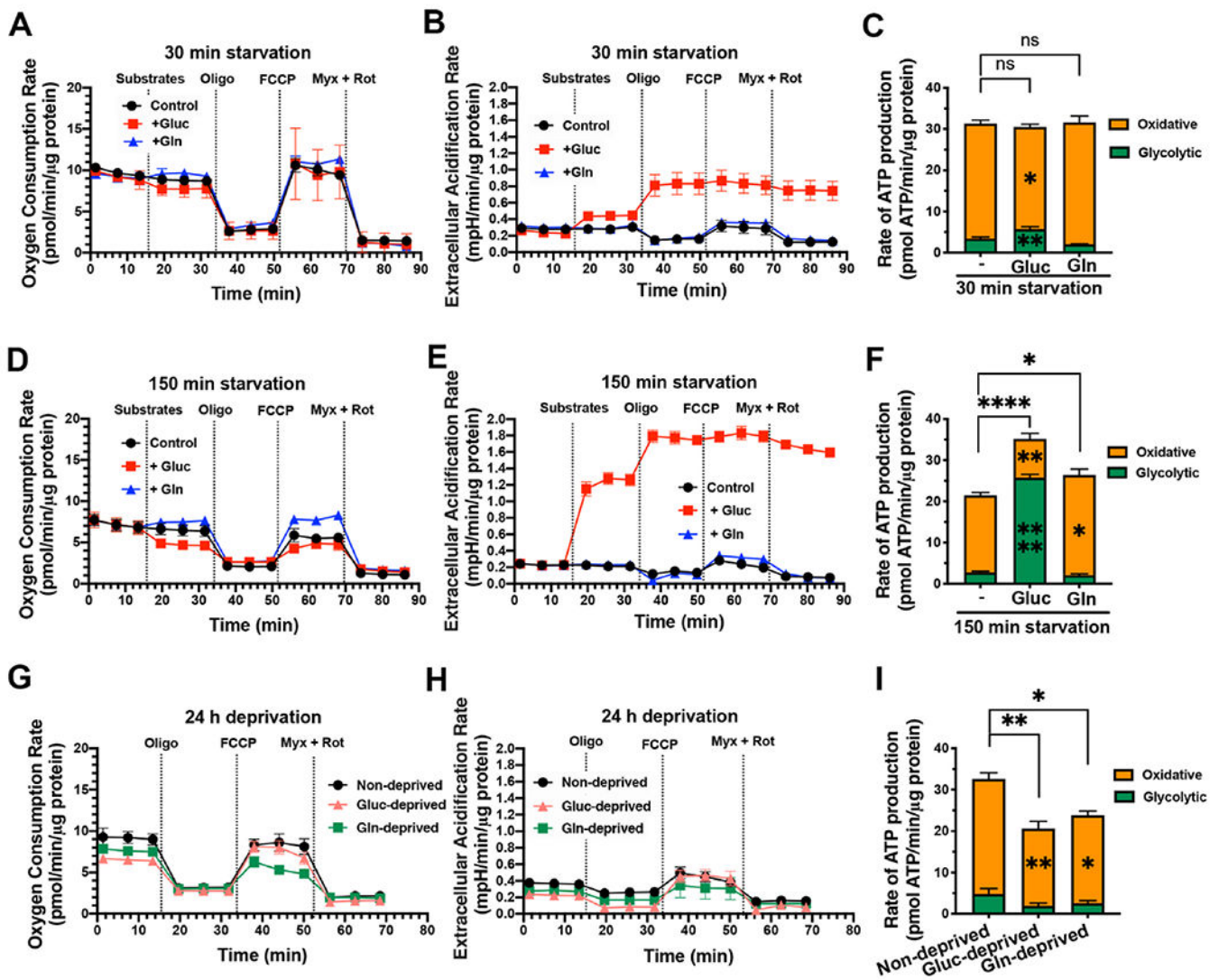


Fig. 4. Effects of addition of glucose and glutamine on the rate of ATP production in 30-min-starved, 150-min-starved and 24-h-deprived AML12 cells. (A–C) 30-min-starved cells; (D–F) 150-min-starved cells; (G–I) 24-h glucose- or glutamine-deprived cells. (A, D, G) Oxygen consumption rate (OCR); (B, E, H) extracellular acidification rate (ECAR); (C, F, I) total and pathway-dependent rates of ATP production just before addition of oligomycin calculated from OCR, ECAR and the buffering power of the medium, as described in Ref. [42] and Section 2.6. Values are means \pm SEM ($N = 3$ independent experiments each the mean of three biological replicates). Port additions where indicated were Substrates: control (vehicle), 25 mM glucose (Gluc) or 10 mM glutamine (Gln); Oligo, 2 μ M oligomycin; FCCP: 2 μ M FCCP; Myx + Rot: 1 μ M myxothiazol plus 1 μ M rotenone.

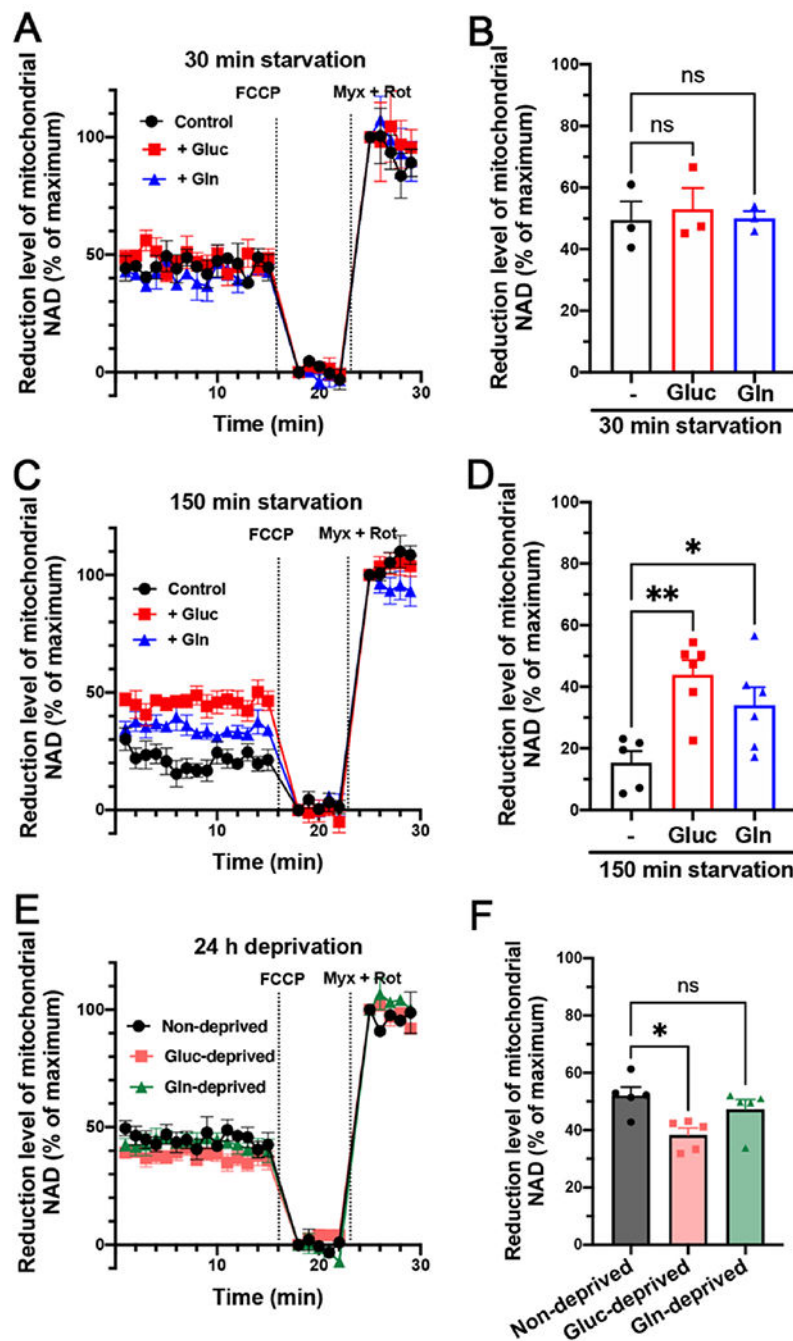


Fig. 5. Effects of glucose and glutamine on the reduction level of mitochondrial NAD. (A, B) 30-min-starved cells; (C, D) 150-min-starved cells; (E, F) 24-h non-deprived and glucose (or glutamine) deprived cells. Vehicle, 25 mM glucose (Gluc) or 10 mM glutamine (Gln) was added at the start of each run in A and C. Additions where indicated were 2 μ M FCCP to define 0% reduced and 1 μ M myxothiazol plus 1 μ M rotenone to define 100% reduced. Each point in B, D and F represents the mean reduction state over 15 min before FCCP

addition. All values are means \pm SEM (N = 3 independent experiments each the mean of three biological replicates).

Author Manuscript

Author Manuscript

Author Manuscript

Author Manuscript

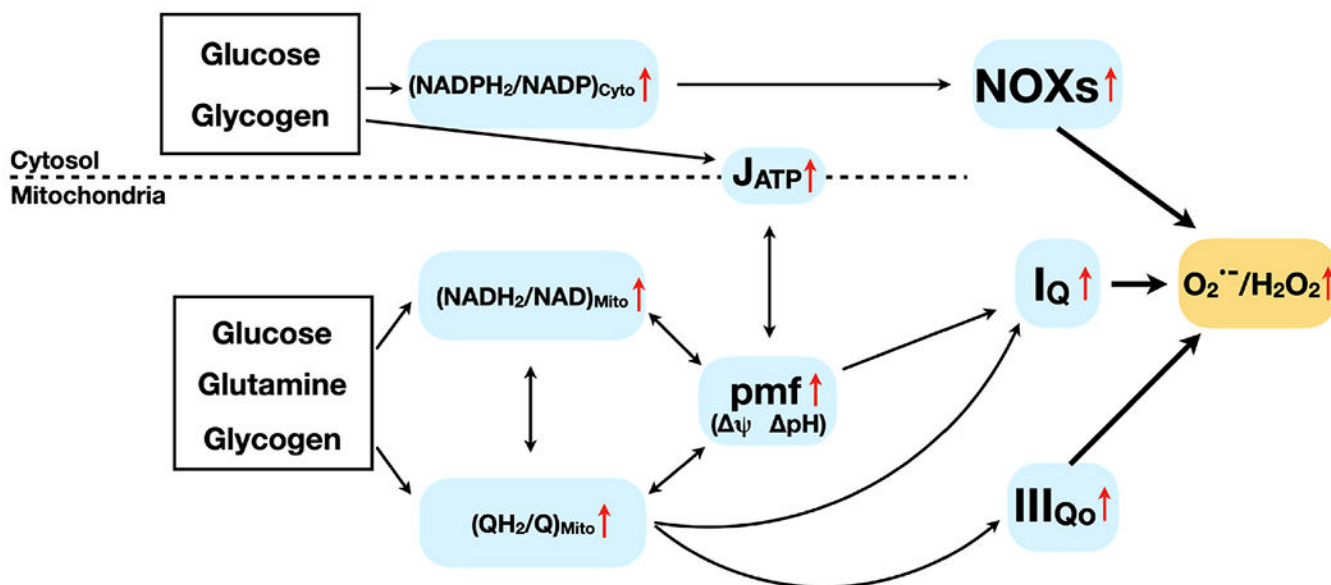


Fig. 6.

Model for the mechanisms by which glucose and glutamine induce hydrogen peroxide release from AML12 cells. In non-starved cells, endogenous substrates such as glycogen are sufficient to keep cytosolic NADP reduced and drive cytosolic NOXs to generate about 45% of the total hydrogen peroxide released by the cells. These endogenous substrates are also sufficient to keep the mitochondrial NAD and Q-pools reduced and drive the generation of protonmotive force (pmf) and maintain high rates of ATP synthesis (J_{ATP}). The strong reduction of the NAD and Q-pools and the high protonmotive force drive superoxide and hydrogen peroxide from sites I_Q and III_{Qo} of the electron transport chain, to generate 35–40% of the total hydrogen peroxide released by the cells. Site I_Q is also driven by the high pH across the mitochondrial inner membrane, whereas site III_{Qo} is depressed by the membrane potential (Ψ). Acute addition of substrates to 30-min-starved cells has little effect on hydrogen peroxide release, ATP production or NAD reduction level because endogenous substrates are already adequate. In cells acutely starved for 150 min, the levels of glycogen and other endogenous substrates drop, compromising the reduction of the NADP, NAD and Q-pools and the consequent production of ATP and release of hydrogen peroxide. In these cells, acute addition of glucose (and to some extent glutamine), but not fructose, palmitate, leucine or alanine, partially reverses these effects and mostly restores ATP production, NAD reduction level and hydrogen peroxide release emanating from NOXs, site I_Q and site III_{Qo} .